Template-Grown Metal Nanowires as Resonators: Performance and Characterization of Dissipative and Elastic Properties

Mingwei Li,[†] Theresa S. Mayer,[†] James A. Sioss,[‡] Christine D. Keating,[‡] and Rustom B. Bhiladvala*,[†,§]

Department of Electrical Engineering, Department of Chemistry, Materials Research Institute, The Pennsylvania State University, University Park, Pennsylvania 16802

Received June 13, 2007; Revised Manuscript Received August 22, 2007

ABSTRACT

Metal resonators can significantly extend the scope of nanoelectromechanical systems (NEMS) through access to a broader range of electrical, thermal, and surface properties. The material behavior of template-electrodeposited gold (Au) and rhodium (Rh) nanowires (NWs) and their performance as resonators was investigated. Nanowire integration by a bottom-up assembly scheme enabled creation of fixed-free metal beams without distortion or tension. Surprisingly, even a soft metal such as Au yielded viable nanocantilever resonators, with *Q*-factors of 600−950 in high vacuum, while stiffer RhNW had *Q*-factors of 1100−1300. NWs with diameter ∼300 nm yield Young's modulus values of 44 ± 12 GPa for Au and 222 ± 70 GPa for Rh, both lower than bulk values. This observation is in agreement with two other measurement techniques.

Resonant nanoelectromechanical systems (NEMS) have a high ratio of resonance frequency to mass, which has been reported to yield mass sensitivity into the zeptogram range,[1] suitable for weighing small numbers of viruses[2] or atoms of metal[3] or inert gas.[1] NEMS devices such as nanowires (NWs) or nanotubes have also been proposed as sensors for a variety of applications[4] and as model systems for exploring quantum phenomena,[5] rarefied gas dynamics,[6] and mechanical properties[7] of materials synthesized by new techniques.[8−10] For nanoscale resonators made entirely from metals, there is little work with quantitative information about intrinsic material properties such as the material's Young's modulus, which determines the effective stiffness, and the *Q*-factor, which yields information on the dissipative characteristics. Metal resonators can extend NEMS applications by expanding the range of physical and chemical properties available, e.g., high electrical/thermal conductivity, range of density and elastic modulus, and little or no native surface oxide formation for noble metals. In addition, well-established surface functionalization chemistries[11] for some metals enable selective binding of targets for sensing.

Despite these attractive features, few room-temperature studies of nanoresonators containing metals[12,13] have been reported. There appear to be two main reasons. First, it is difficult to control distortion (of cantilevers) or residual tension (of doubly clamped structures) arising from metal film stress during the releasing etch of the sacrificial layer in top-down fabrication of nanostructures made from metal films.[14,15] Second, data on thin-film nanoscale resonators made entirely of metal (100 nm thick Al)[12] or of a continuous thin layer of metal on single-crystal silicon (15 nm Al on 200 nm thick Si)[13] indicate significant effects of energy dissipation on performance, with low *Q*-factor values (∼200), which reduces the potential for many device applications. In this letter, we describe distortion-free cantilevered resonators made from metal NWs using a recently developed hybrid bottom-up integration technique.[16] Although resonance peak frequency (*f*) and *Q*-factor (*Q*) are performance attributes for resonator applications, they also serve as data for the characterization of elastic and dissipative properties of resonator material. Choices that yield higher *f* and *Q*, such as the use of stiffer doubly clamped nanobeams in place of nanocantilevers or the use of tension in doubly clamped beams,[17,18] enhance resonator performance but create additional sources of uncertainty during material characterization. Hence the ability to perform experiments with tension- and distortion-free cantilevered metal NWs, enabled by this integration technique, is important for characterizing NW material behavior.

To examine whether a relatively soft, pliable, low-melting-point metal such as gold (mp = 1063 °C) is too dissipative

---

* Corresponding author. E-mail: rbb16@psu.edu.
† Department of Electrical Engineering.
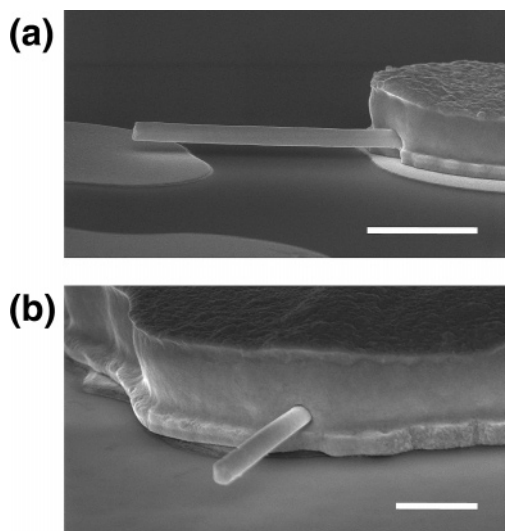‡ Department of Chemistry.
§ Materials Research Institute.

Figure 1. Scanning electron micrographs of Au nanowire (NW) cantilever resonators. (a) Oblique view of a Au NW with $l = 4.7$ μm, $d = 340$ nm. (b) Near head-on view of a Au NW with $l = 2.4$ μm, $d = 260$ nm, showing the thickness and intimate contact of clamp metal completely surrounding the NW. Scale bars are 2 and 1 μm, respectively.

to yield viable resonant nanocantilevers, we selected template-electrodeposited gold (Au) NWs. For comparison, we studied NWs of similar dimensions, made from rhodium (Rh), known to have relevant characteristics similar to Au, but with a higher stiffness (modulus $E_{Rh} = 4.6$ E_{Au} for bulk material) and melting point (mp = 1965 °C).

Au or Rh NWs were synthesized as previously described[16,19−22] by electrodeposition of metal from plating solutions (Orotemp for Au, Rhodium S-Less for Rh, both from Technic, Inc.) within an anodic aluminum oxide (AAO) template (Anodisc25, nominal pore size 0.2 μm, from Whatman) using a constant current of 1.65 mA. NWs were released into suspension by dissolving the template in a 3.0 M NaOH solution. NWs with diameter ∼300 nm, some with measured taper, were obtained, with lengths from 5 to 10 μm, controlled by varying electrodeposition time. On the basis of recent high-resolution transmission electron microscopy (HRTEM) studies,[21,22] both Au and Rh NWs may be expected to be polycrystalline. High-melting-point materials such as Rh have higher metal−metal bond energies[20] and smaller grain size than low-melting-point materials such as Au,[22] for which grains spanning the NW diameter have been reported.[21]

The bottom-up scheme for integrating arrays of NW cantilevers is detailed elsewhere.[16] In this integration scheme, a dielectrophoretic assembly step was designed to enable controlled in-plane location and suspension height of NWs; thick (greater than 1 μm) metal clamps, completely surrounding one or both tips of the suspended NWs were then created by Au electrodeposition. Such clamps should reduce energy losses associated with the support undercut that is obtained by other clamping procedures.[16] Figure 1 shows scanning electron micrographs of Au NW cantilevered resonators suspended 300 nm above the substrate surface. Following fabrication, the chip with NW resonators was
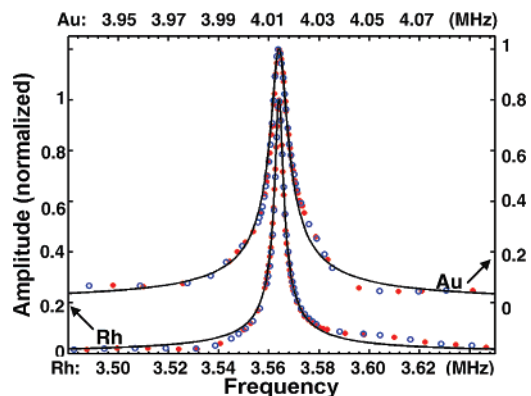

Figure 2. Resonance spectra from cylindrical nanowire cantilevered resonators of Au ($d = 290$ nm, $l = 3.8$ μm, $f = 4.016$ MHz, $Q = 710$) and Rh ($d = 235−345$ nm, tapered, $l = 7.4$ μm, $f = 3.564$ MHz, $Q = 1200$). Measured data (points) are well approximated by a Lorentzian curve (solid line) for an ideal linear harmonic oscillator. The coincidence between sweeps with increasing (red dots) and decreasing (blue dots) frequency shows the absence of stiffness nonlinearity.

mounted on a piezoelectric disk inside a vacuum chamber evacuated to 2×10^{-7} Torr. Resonance signal transduction was achieved using an optical interferometric system.[23]

Resonance spectra for Au and Rh NW resonators in high vacuum at room temperature are shown in Figure 2, plotted with increasing and decreasing frequency sweeps. No hysteresis is observed, indicating the absence of stiffness nonlinearities; the plots are well described by a Lorentzian function, showing linear harmonic resonator behavior. The resonance spectrum for a Au NW ($l = 3.8$ μm, $d = 285$ nm) gives a Q-factor of 710; values for all Au NWs measured range from 600 to 940. The spectrum shown for the Rh NW cantilever (length $l = 7.4$ μm, diameter $d = 235−345$ nm, tapered), yields a Q-factor of 1200; values for all Rh NWs measured range from 1100 to 1300. Q-values up to 1000 for NW cantilevers have been observed previously[24] using single-crystal CVD-grown NWs of the semimetal boron, clamped by using electron beam induced deposition (EBID) of hydrocarbons.

A prevalent view is that the use of metallic materials is associated with degradation in Q-value.[13] An early experimental study of dissipation in metallized thin-film nanostructures (Si[13] nanobeams, $w = 170$ nm, $t = 200$ nm, $l = 2$ μm) for a torsional resonator shows a monotonic reduction of Q-factor from ∼3500 to ∼200, when the thickness of Al metal deposited on the beams is increased in steps from 0 to 15 nm. The authors[13] conclude that metallization should be avoided due to the high degradation in Q. A recent study[12] of a cantilevered nanoresonator made by top-down fabrication purely from metal thin film reports $Q \sim 200$ for an evaporated Al nanocantilever (width $w = 400$ nm, thickness $t \approx 100$ nm), with its authors noting some distortion from the fabrication process. Because of the limited metal nanocantilever data available, we estimate an equivalent cantilever Q-factor from doubly clamped nanobeam data, which show measured $Q \sim 1300$ in each of two recent nanoresonator studies: (i) with 40 nm thick Cr on Si[23] nanobeams ($w = 900$ nm, $t = 219$ nm, $l = 8.5$ μm) and (ii) with 100 nm

thick Al on Si nitride[25] nanobeams ($w = 200$ nm, $t = 125$ nm, $l = 14 \mu$m). For a nanobeam modeled as a linear, single-degree-of-freedom harmonic oscillator with Q much greater than 1, $Q = 2\pi Mf C^{-1} = (MK)^{1/2} C^{-1}$, with the coefficients for mass (M), stiffness (K) and damping (C) independent of displacement amplitude. Doubly clamped and cantilevered nanobeams of the same material and dimensions have the same mass; we assume, for small energy losses through clamps, that the damping coefficient C is roughly the same for the two cases, independent of the mode shape. Under this assumption, a rough estimate for an equivalent nanocantilever Q-value may be obtained by multiplying the doubly clamped Q-value by the ratio of resonant frequencies, ($f_{cant}/f_{dblclmpd}$), which reduces simply to the ratio of the squares of modal constants (β in eq 1), a factor 0.16 ($=1.88^2/4.73^2$). If the measured frequency $f_{dbl-clmpd}$ includes a tension-induced increase by a factor r over the unstressed doubly clamped beam value, the estimate for equivalent nanocantilever Q should be further reduced by a factor ($1/r$); conservatively, we have assumed $r = 1$. This yields an equivalent nanocantilever $Q \sim 200$ for (i) and (ii). Taken together, the available data indicate low $Q \sim 200$ for thin-film nanocantilevers made of metal or metallized with film thicknesses >15 nm of either Al or Cr. The prevalent view[13] that use of metals or metallized materials is associated with degradation in nanocantilever Q-values at room temperature, seems supported by data from thin-film-etched nanostructures made by top-down methods. This view is, however, contradicted by data from experiments with cantilevered NWs of Au and Rh presented here, as well as by earlier data from cantilevered NWs of the semi-metal boron.[24]

The difference in Q-values between NWs and thin-film (TF) etched cantilevers could result from the effect of TF cross-section geometry on stiffness, if the aspect ratio of the TF cross-section is high, but is not significant for the small aspect-ratio TF cross-sections discussed here. Significant oxidation of (and dissipation in) the metal film used is a factor to be considered for materials such as Al,[12,13] in contrast to Au and Rh. Compared to the clamped, electrode-posited metal NWs, metal nanostructures patterned from evaporated thin film may dissipate more energy during flexure due to a higher volume fraction of grain boundaries or defects or have higher dispersive anchor losses;[26,27] these factors will require a comparative study of both NW and TF resonators, including grain morphology. However, other factors that could explain the lower Q-values reported for metal(lized) TF nanocantilevers include energy dissipation due to undercuts[12] and dry-etch-damaged surface,[28] which are absent in the metal NW cantilevers studied here.

The reduction of uncertainties from beam tension, undercuts and surface damage in the arrays of cantilevered NW resonators shown here constitute a significant step toward the goal of characterizing the inherent "lossiness" of materials as synthesized. This may be done by obtaining an average value of damping coefficient C over an array of NWs of the same dimensions to characterize dissipative behavior for each material, thus enabling comparison of different materials.
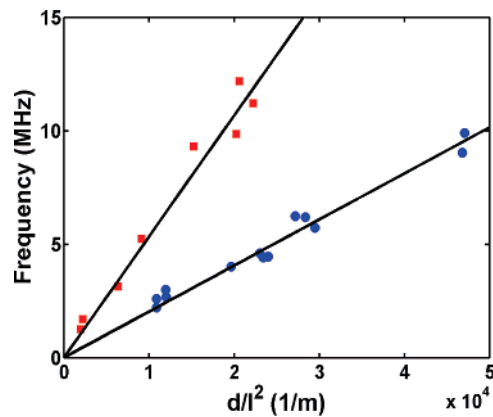
Figure 3. Scaling dependence of the resonance frequency of Au and Rh nanowires on geometry (linear with d/l^2). Measured resonant frequencies from 13 Au nanowires (blue circles) and 8 Rh NWs (red squares) are in accord with Euler−Bernoulli beam theory, eq 1. Solid lines are best fits to this data, and the mean of Young's modulus values calculated for each batch of NWs was 44 GPa for Au and 222 GPa for Rh.

To characterize elastic behavior using flexural vibration of a cantilevered cylindrical beam modeled as a harmonic oscillator in a low damping environment (high vacuum), we use the expression for resonance frequency,[24]

$$f = \frac{\beta^2}{8\pi} \sqrt{\frac{E}{\rho}} \frac{d}{l^2} \tag{1}$$

where E, ρ, d, and l are the Young's modulus, density, diameter, and suspension length, respectively. Using measured values of fundamental mode frequency f_0, d, l (see table in Supporting Information), and bulk values for ρ, we obtain values of E from eq 1, using the assumption of a rigid clamp, for which modal constant $\beta = 1.88$.[16] For NWs with taper arising from template pores, we used a modified model that accounts for varying beam cross section[29] for extracting the modulus value. Resonance frequencies f are plotted against d/l^2 in Figure 3, yielding Young's modulus values 44 ± 12 GPa (range 30−72 GPa), 54% of the value 82 GPa quoted for bulk polycrystalline Au,[30] and 222 ± 70 GPa (range 150−375 GPa) for the Rh NWs, 59% of 379 GPa quoted for bulk polycrystalline Rh.[30] In a related study[16] of Si NWs produced by the same bottom-up fabrication technique used here, we observed low scatter in a data plot of f against d/l^2, establishing that the clamps are of repeatable rigidity. Here, geometry measurement by scanning electron microscopy contributes small uncertainties ($\pm4\%$ total, from both l and d). Significant variation in density and modulus across NWs grown in the same template is unlikely, suggesting that the main contributions to the scatter in our metal NW modulus data are due to observed deviations from cylindrical geometry (such as a slight barreling or waist along NW length) attributable to the geometry of the nanopores in the templates used. Large scatter is also reported in the AFM study[21] of Young's modulus of Au NWs grown using nanoporous templates from the same source.

Young's modulus values obtained[21] through the AFM-measured deflection for doubly clamped polycrystalline

electrodeposited Au NWs are 70 ± 11 GPa (range $40-107$ GPa) for $40-250$ nm diameter wires.[21] Modulus measurements by Hartland and co-workers,[10] use much smaller single-crystal Au NWs of diameters $5-25$ nm and lengths $20-85$ nm, produced by seed-mediated growth, with acoustic velocity of groups of NWs measured by a novel spectroscopic method. They report values of 31 ± 1 GPa (range $22-39$ GPa) for [100] Au NWs compared to bulk $E_{[100]} = 42$ GPa, and 64 ± 2 GPa for [110] Au NWs compared to bulk $E_{[110]} = 81$ GPa. No published modulus values of Rh NWs for comparison are known to us. We observe that all three measurement methods for Au NWs, spanning a large diameter range, yield modulus values lower than those quoted for bulk material. Crystal orientation or grain morphology, defect distribution, nanostructure size, and growth/fabrication method may each need to be tracked in experiments before materials for nanoresonators can be labeled, and a correlation of results from several measurement techniques needed to unambiguously associate property values to the materials labeled.

In conclusion, distortion-free metal nanocantilevers have been made by bottom-up assembly of template-grown NWs. Unlike doubly clamped metal nanobeams, such metal nanocantilevers are difficult to make by top-down methods. These cantilevered NW resonators, with individual thick metal clamps surrounding the NW end, allow quantification of material mechanical characteristics without the effects of support undercut and the tension-induced uncertainties associated with doubly clamped beams. Room-temperature measurements in vacuum show that even a soft, low melting point metal such as Au can yield viable nanocantilever resonators, with Q up to 950, while stiffer, higher-melting-point Rh NWs yield Q up to 1300. In agreement with two other measurement techniques, elastic (Young's) modulus values obtained by our method are lower than quoted values for bulk material. The techniques used here may be applied to NWs synthesized by any technique. Finally, material characterization procedures closest to NEMS operating procedures may be helpful until measurement process dependencies are sorted out, making the techniques here particularly suited to material characterization for the design of practical devices based on metallic NEMS resonators.

Supporting Information Available: Evaluation of Young's modulus (E) from 8 Rh nanowires and 13 Au nanowires. This material is available free of charge via the Internet at http://pubs.acs.org.

References

(1) Yang, Y. T.; Callegari, C.; Feng, X. L.; Ekinci, K. L.; Roukes, M. L. *Nano Lett.* **2006**, *6*, 583.
(2) Ilic, B.; Yang, Y.; Craighead, H. G. *Appl. Phys. Lett.* **2004**, *85*, 2604.
(3) Ekinci, K. L.; Huang, X. M. H.; Roukes, M. L. *Appl. Phys. Lett.* **2004**, *84*, 4469.
(4) Lavrik, N. V.; Sepaniak, M. J.; Datskos, P. G. *Rev. Sci. Instrum.* **2004**, *75*, 2229.
(5) LaHaye, M. D.; Buu, O.; Camarota, B.; Schwab, K. C. *Science* **2004**, *304*, 74.
(6) Bhiladvala, R. B.; Wang, Z. J. *Phys Rev E* **2004**, *69*.
(7) Poncharal, P.; Wang, Z. L.; Ugarte, D.; de Heer, W. A. *Science* **1999**, *283*, 1513.
(8) Xia, Y. N.; Yang, P. D.; Sun, Y. G.; Wu, Y. Y.; Mayers, B.; Gates, B.; Yin, Y. D.; Kim, F.; Yan, Y. Q. *Adv. Mater.* **2003**, *15*, 353.
(9) Murphy, C. J.; Gole, A. M.; Hunyadi, S. E.; Orendorff, C. J. *Inorg. Chem.* **2006**, *45*, 7544.
(10) Petrova, H.; Perez-Juste, J.; Zhang, Z. Y.; Zhang, J.; Kosel, T.; Hartland, G. V. *J. Mater. Chem.* **2006**, *16*, 3957.
(11) Love, J. C.; Estroff, L. A.; Kriebel, J. K.; Nuzzo, R. G.; Whitesides, G. M. *Chem. Rev.* **2005**, *105*, 1103.
(12) Davis, Z. J.; Boisen, A. *Appl. Phys. Lett.* **2005**, *87*.
(13) Olkhovets, A.; Evoy, S.; Carr, D. W.; Parpia, J. M.; Craighead, H. G. *J. Vac. Sci. Technol., B* **2000**, *18*, 3549.
(14) O'Mahony, C.; Hill, M.; Hughes, P. J.; Lane, W. A. *J. Micromech. Microeng.* **2002**, *12*, 438.
(15) Fang, W.; Wickert, J. A. *J. Micromech. Microeng.* **1996**, *6*, 301.
(16) Li, M.; Bhiladvala, R. B.; Morrow, T. J.; Sioss, J. A.; Lew, K. K.; Redwing, J. M.; Keating, C. D.; Mayer, T. S. Submitted for publication.
(17) Cimmalla, V.; Foerster, Ch.; Will, F.; Tonisch, K.; Brueckner, K.; Stephan, R.; Hein, M. E.; Ambacher, O. *Appl. Phys. Lett.* **2006**, *88*, 253501.
(18) Verbridge, S. S.; Shapiro, D. F.; Craighead, H. G.; Parpia, J. M. *Nano Lett.* **2007**, *7*, 1728.
(19) Nicewarner-Pena, S. R.; Freeman, R. G.; Reiss, B. D.; He, L.; Pena, D. J.; Walton, I. D.; Cromer, R.; Keating, C. D.; Natan, M. J. *Science* **2001**, *294*, 137.
(20) Kline, T. R.; Tian, M. L.; Wang, J. G.; Sen, A.; Chan, M. W. H.; Mallouk, T. E. *Inorg. Chem.* **2006**, *45*, 7555.
(21) Wu, B.; Heidelberg, A.; Boland, J. J. *Nat. Mater.* **2005**, *4*, 525.
(22) Tian, M. L.; Wang, J. U.; Kurtz, J.; Mallouk, T. E.; Chan, M. H. W. *Nano Lett.* **2003**, *3*, 919.
(23) Kouh, T.; Karabacak, D.; Kim, D. H.; Ekinci, K. L. *Appl. Phys. Lett.* **2005**, *86*, 013106.
(24) Ding, W. Q.; Calabri, L.; Chen, X. Q.; Kohlhaas, K. M.; Ruoff, R. S. *Compos. Sci. Technol.* **2006**, *66*, 1112.
(25) Kouh, T.; Basarir, O.; Ekinci, K. L. *Appl. Phys. Lett.* **2005**, *87*, 113112.
(26) Photiadis, D. M.; Judge, J. A. *Appl. Phys. Lett.* **2004**, *85*, 482.
(27) Harrington, D. A.; Mohanty, P.; Roukes, M. L. *Physica B* **2000**, *284*, 2145.
(28) Mihailovich, R. E.; MacDonald, N. C. *Sens. Actuators A, Phys.* **1995**, *50*, 199.
(29) Chen, X. Q.; Zhang, S. L.; Wagner, G. J.; Ding, W. Q.; Ruoff, R. S. *J. Appl. Phys.* **2004**, *95*, 4823.
(30) *ASM Handbook Volume 8, Mechanical Testing and Evaluation*; The Materials Information Society: Materials Park, Ohio, 1990; p 938.

NL071416E